JOURNAL OF CATALYSIS 139, 561–567 (1993)

Evidence for Low-Temperature Oxygen Migration from Ceria to Rh

G. S. ZAFIRIS AND R. J. GORTE

Department of Chemical Engineering, University of Pennsylvania, Philadelphia, Pennsylvania 19104

Received May 14, 1992; revised September 21, 1992

We have examined the structure and adsorption properties Rh deposited on amorphous ceria films in ultrahigh vacuum. Following adsorption of CO on Rh/ceria, a significant fraction of the CO reacts to CO_2 during temperature-programmed desorption (TPD), even for relatively large Rh particles. The extra oxygen is shown to come from the ceria, since the near-surface region can be depleted by multiple adsorption–desorption cycles and since additional oxygen can be brought out from the bulk ceria by high-temperature annealing. The adsorption of NO on Rh/ceria is also affected in ways that suggest that the oxygen is migrating to the surface of the Rh near room temperature. These results have important implications on the catalytic properties of Rh/ceria catalysts and help to explain the high activity of these catalysts for the water–gas-shift reaction.

INTRODUCTION

The simultaneous reduction of NO and oxidation of CO and hydrocarbons in the three-way, automotive catalyst require that the catalyst have rather remarkable performance capabilities. The best catalysts for these reactions contain mainly Pt, Pd, and Rh as their primary, active components; but other species, including ceria, are also added to enhance catalytic performance. There appear to be a number of reasons why ceria-containing catalysts are better, although which of the proposed features are most important is uncertain. Among the first suggestions was that ceria provides oxygen-storage capacity during lean operating conditions (*1–3*). Other proposals include that ceria may change the properties of the Group VIII metals through electronic interactions (*4, 5*) and that the presence of ceria may improve the thermal stability of the support, maintaining the surface area of alumina under harsh treatment conditions (*6*). Finally, it was reported that ceria and, in particular, Rh/ceria, is an excellent water–gas-shift catalyst, which could aid in the removal of CO, especially at low temperatures (*7–9*). This reaction would also produce H_2 which could further assist in the reduction of NO.

In a previous paper, we showed that interactions between Pt and ceria are relatively weak, and ceria-supported particles were found to exhibit very similar adsorption properties to alumina-supported Pt for CO, H_2, and NO (*10*). In contrast, we demonstrate here that the interactions between Rh and CeO_2 are much stronger and oxygen is able to migrate from the ceria onto supported Rh particles.

Temperature-programmed desorption (TPD) measurements of CO show substantial desorption of CO_2, and TPD curves for NO also show features which may be attributable to coadsorbed oxygen. The migration of oxygen from the ceria support onto Rh can be used to explain the high activity that this catalyst has for the water–gas-shift reaction.

EXPERIMENTAL SECTION

Ceria films were prepared by spray pyrolysis of a 0.1 *N* aqueous solution of $Ce(NO_3)_3$ (99.5% purity, Johnson & Matthey) onto either an α-Al_2O_3(0001) or an NaCl substrate held between 600 and 670 K in air. The solution was sprayed at a flow rate of 2 ml solu-

0021-9517/93 $5.00

tion/min for 15 min using N_2 as the carrier. Following deposition, the samples were kept at 650 K for an additional 25 min. The cycle was repeated four times to produce a film approximately 10 μm thick. Finally, the samples were heated overnight in air at 500 K. In order to characterize the films, transmission electron microscopy (TEM) was performed on the films grown on the NaCl substrates. Microscopy samples were prepared by dissolving the NaCl in distilled water and placing the film onto an Au specimen grid. Measurements were carried out on a Philips EM400T microscope, with the results showing that the films were amorphous, with a thickness that varied significantly over the sample.

The TPD measurements were performed in a standard, ultrahigh-vacuum chamber which had a base pressure $\sim 2 \times 10^{-10}$ Torr and has been described previously (*10, 11*). Briefly, the chamber is equipped with an Auger electron spectrometer (AES), a metal source for Rh deposition, and a quartz crystal film thickness monitor for measuring the metal coverage. A cone around the quadrupole mass spectrometer enhance desorption from the sample and minimized desorption from the sample leads. The α-Al_2O_3(0001)-supported sample, used in all of the surface measurements, was mounted on a resistively heated, tantalum foil, which allowed the sample to be heated to 950 K. The temperature was monitored using a chromel–alumel thermocouple attached to the back side of the crystal using a UHV-compatible, ceramic adhesive. (Previous work has demonstrated that the temperatures measure in this way are accurate and that gradients in the crystal are insignificant (*10, 12, 13*). After cleaning the sample by ion bombardment and heating at 850 K in 1×10^{-7} Torr of O_2, AES showed only cerium, oxygen, and traces of chlorine. (The Cl(181 eV)/O(508 eV) was always less than 0.03, which we consider to be very small based on the fact that the Cl(181 eV) signal is significantly more sensitive than that for O(508 eV) (*25*).) The TPD experiments were carried out using a heating rate of $\sim$4 K/sec, and ^{15}NO was used for the NO desorption measurements in order to distinguish N_2 and N_2O from possible CO and CO_2 contamination. In order to remove the adsorbed oxygen resulting from the NO decomposition, the sample was heated in 1×10^{-7} Torr H_2 at 850 K after each NO TPD. The mass spectrometer was multiplexed to a personal computer for simultaneous detection of several masses.

In all of the experiments, Rh was first vapor deposited onto the ceria film at room temperature. A plot of the AES peak intensities for the Rh(302 eV) and O(510 eV) peaks as a function of coverage, determined from the film-thickness monitor, was essentially identical to that obtained for Rh on ZrO_2(100) (*11*), which indicates that the as-deposited Rh film is close to two dimensional. Upon heating, there is a decrease in the Rh(302-eV) peak, an increase in the O(510-eV) peak, and decrease in the adsorption capacity. These observations indicate either that the film agglomerates into particles or that there is migration of the Rh into the ceria. Estimates of the particle size for the annealed films, calculated from the metal coverage and the CO adsorption capacity, assuming one CO per surface Rh, gave diameters of 6 nm for 0.25×10^{15} Rh/cm^2, 14 nm for 1×10^{15} Rh/cm^2, and 15 nm for 5.5×10^{15} Rh/cm^2. These diameters are reasonable, but larger than expected based on the same metal coverages on other oxide substrates (*11–13*). There may be migration of a small amount of oxide onto the Rh particles, such as has been suggested for lanthana on Pd (*14*), although the extent to which this occurs must be limited.

RESULTS

CO Adsorption

The TPD curves for CO from as-deposited, unannealed Rh films at two metal coverages are shown in Fig. 1, along with a TPD curve from the clean ceria for comparison. The metal coverages were 5.5×10^{15} and 1×10^{15} Rh/cm^2, which corresponds to cov-

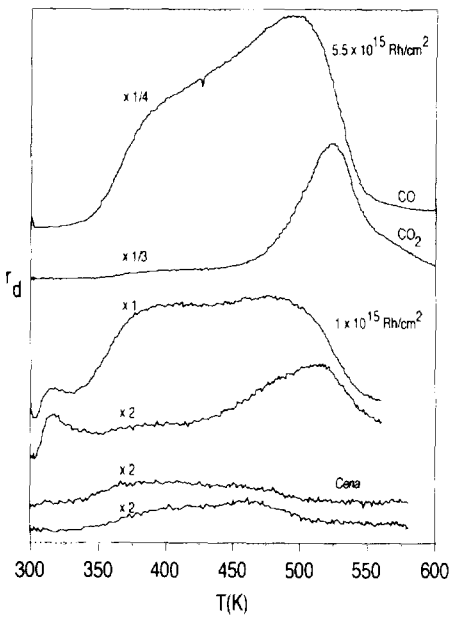

FIG. 1. Saturation TPD curves following CO adsorption on Rh films which had been freshly deposited onto ceria at 300 K. The Rh coverages are given in the figure.

erages of approximately five and one monolayer, respectively. What is immediately apparent is that a considerable amount of the CO desorbs as CO_2 in a peak centered at ~520 K, ~20% by peak area, even for the five-monolayer film. We observed no evidence for carbon deposition in our studies, showing that the CO_2 must be formed by the presence of oxygen on the Rh. It is interesting that there is very little reaction to CO_2 prior to 400 K. If oxygen had been coadsorbed with CO at room temperature, one should expect to see reaction to CO_2 at lower temperatures. This implies that the oxygen must be introduced to the Rh during the TPD run, beginning at ~400 K. The CO curves are also consistent with this picture of oxygen being introduced to the surface during the TPD measurement. The curves show two peaks at 410 and 480 K, similar to what is found in TPD curves for CO from both Rh particles, single crystals, and foils (*11, 13, 15–18*). However, the high-temperature feature from bulk Rh is usually much larger than the low-temperature feature, except for very small Rh particles, while the two features are almost equal in size in Fig. 1. Since CO_2 forms in this same temperature region, the high-temperature feature is probably reduced in size by the reaction.

TPD measurements for subsequent CO exposures are shown in Fig. 2 for the Rh coverage of 1×10^{15}Rh/cm^2, the same Rh layer shown in Fig. 1b. Unless otherwise noted, we stopped the heating ramp at 560 K in order to minimize movement of oxygen in the ceria, assuming that ceria is the source of the oxygen which reacts with the CO. In the second TPD curve obtained for this Rh film, shown in Fig. 2a, we again observed significant desorption of CO_2, ~30% of the CO peak area; however, a second, low-temperature, CO_2 peak is observed in Fig. 2a at 390 K, in addition to the high-temperature CO_2 peak. Also, the ratio of the high-tem-

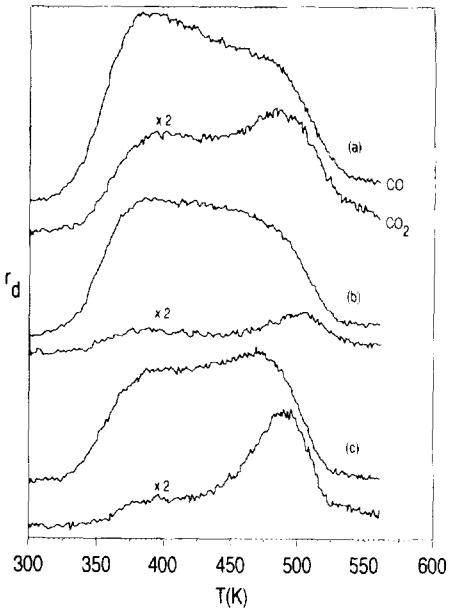

FIG. 2. Saturation TPD curves for CO from the Rh film containing 1×10^{15} Rh/cm^2: (a) immediately after cooling the sample in Fig. 1b from 560 K; b) after eight successive TPD measurements with CO, with the sample having been heated to only 560 K for all but the third TPD; and (c) after heating the sample in (b) to 920 K in vacuum.

perature feature for CO to the low-temperature feature is decreased even further than was observed on the as-deposited film. What these results suggest is that oxygen is already coadsorbed with CO at the beginning of the TPD measurement. Since results for the as-deposited films appear to indicate that oxygen does not interact with CO on the Rh until ~400 K, we suggest that, following the initial TPD measurement, oxygen migrates from the ceria onto the Rh as the sample is cooling from 560 K to room temperature. The TPD curve in Fig. 2a is therefore the result expected for coadsorption of CO and oxygen (*15*).

If the oxygen responsible for CO_2 formation is derived from the ceria, it should be possible to deplete this oxygen with multiple adsorption–desorption cycles of CO. Since oxygen is very mobile in ceria at elevated temperatures, high-temperature annealing of a sample which had been prereduced at the surface should increase the CO_2 formation. Figure 2b shows the same sample as in Fig. 2a after eight successive TPD measurements with CO, with the sample having been heated to only 560 K for all but the third TPD, when it was heated to 920 K. Only a small amount of CO_2 desorption (~10% of the CO peak) is observed, although the relative size of the low- and high-temperature CO peaks is higher than would be expected for large Rh particles (The particle size was estimated to be ~14 nm based on the adsorption capacity.). Heating this surface to 920 K brings oxygen back to the surface of the ceria and increases the amount of CO_2 that is formed. In Fig. 2c, we show the TPD curve obtained from the sample in Fig. 2b after it had been heated to 920 K for 3 min. The fraction of the peak area for the CO_2 is now ~22% of the CO peak area. The amount of CO_2 formed in each of the TPD runs on this sample has been summarized in Fig. 3.

The results discussed in Figs. 2 and 3 were obtained for an Rh coverage of 1×10^{15} Rh/cm^2, which, after annealing to 600 K, gave an average particle size of ~14 nm. Similar measurements were performed for

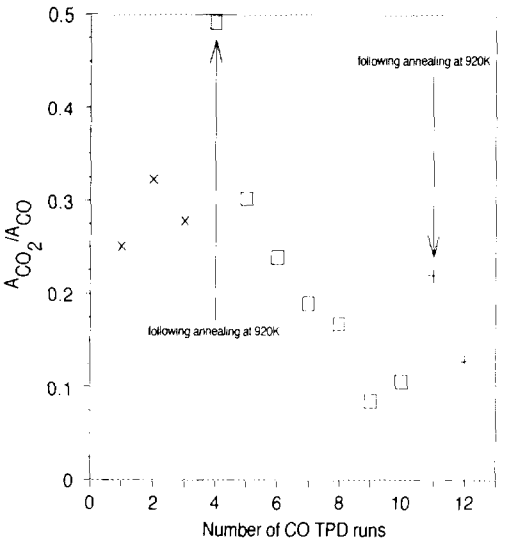

FIG. 3. A plot of the CO_2 peak area divided by the CO peak area for saturation coverages of CO on an Rh film with 1×10^{15} Rh/cm^2 as a function of the number of adsorption–desorption cycles performed on that sample. Except for the measurements indicated by arrows, the sample was heated to only 560 K following each TPD measurement.

metal coverages of 0.25×10^{15} and 5.5×10^{15} Rh/cm^2, for which the particle sizes were estimated to be 6 and 15 nm, respectively, after annealing. These surfaces showed very similar reactivities for CO oxidation to CO_2 during TPD. The fact that changes in particle size and metal coverage did not substantially affect the formation of CO_2 implies that reaction cannot simply occur at the periphery of the Rh particles. Oxygen must migrate from the ceria onto the Rh particles or otherwise affect the entire Rh surface. The particles themselves do not appear to be totally oxidized, although the possibility that they could be partially oxidized is consistent with changes in the relative peak heights of the two CO desorption features, noted above, for particles this large.

NO Adsorption

Due to the importance of Rh for the reduction of NO, we also examined ^{15}NO adsorption on these model catalysts. The TPD

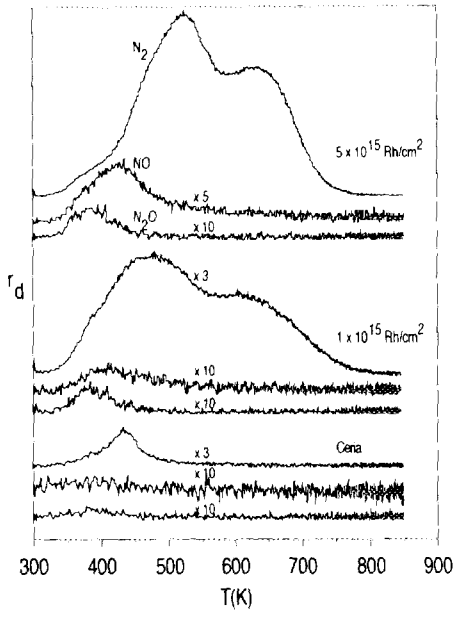

FIG. 4. Saturation TPD curves following NO adsorption on Rh films which had been freshly deposited onto ceria at 300 K. The Rh coverages are given in the figure.

curves following room temperature adsorption for the as-deposited films are shown in Fig. 4 for Rh coverages of 5×10^{15} and 1×10^{15} Rh/cm^2, along with results for the clean ceria. Masses corresponding to N_2, NO, O_2, and N_2O were monitored during the TPD experiment. No O_2 desorption was detected up to 850 K, so that it was necessary to reduce the Rh with H_2 prior to subsequent desorption measurements. For 5×10^{15} Rh/cm^2, approximately 95% of the NO dissociated to N_2 in two features at 520 and 630 K, with another ~5% desorbing as N_2O at ~380 K. Results for 1×10^{15} Rh/cm^2 were essentially the same, although somewhat more of the NO desorbs as N_2 and the N_2 desorption features are shifted downward by ~30 K. The amount of NO which adsorbed on the ceria was small and most of this (~99%) dissociated to N_2 in a peak at 440 K. Since previous results for Rh on ZrO_2(100) showed that unannealed films can exhibit modified desorption curves (*11*), possibly due to structural changes in the film during the desorption process, it is difficult to interpret the results for the as-deposited films.

However, the desorption features on the annealed films are still significantly different from that observed for NO from either bulk Rh or Rh particles supported on ZrO_2(100) or α-Al_2O_3(0001) (*11*, *12*, *15*, *16*, *19–21*). A comparison of results for the annealed Rh/ceria and Rh/ZrO_2(100) surfaces for a coverage of 5×10^{15} is shown in Fig. 5. On both samples, most of the NO dissociated to desorb as N_2. For Rh particles on ZrO_2(100) or α-Al_2O_3(0001), small particles (<6 nm) exhibit a single, N_2 desorption feature at ~580 K while larger particles also show a second, very sharp desorption feature at ~440 K. The sharp peak at 440 K is reported for all Rh single crystals that have been investigated and has been assigned to the reaction of $NO_{ad} + N_{ad}$ to form $N_2 + O_{ad}$ (*19–21*). For Rh particles on ceria, the TPD curve appears to be entirely different. The curves on both large and small particles show two N_2 peaks; but the high-tempera-

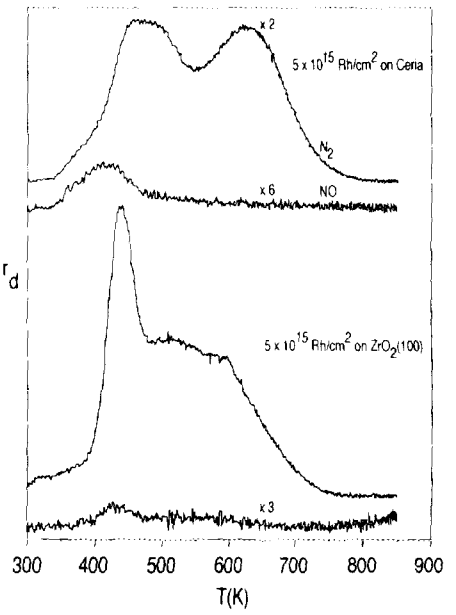

FIG. 5. Saturation TPD curves for NO from annealed films of Rh on ceria and ZrO_2(001). The results for Rh on ZrO_2(100) are given in detail in Ref. (*11*).

ture state is centered at ~630 K and the low-temperature state is broad and shifted to higher temperatures, between 470 and 510 K.

Since the Rh particles on the Rh/ceria are quite large (~15 nm), it is difficult to explain these results as due to electronic interactions between Rh and ceria. A clue to the NO desorption results from this sample may come from previous coadsorption measurements with NO and O_2 on both Rh particles and single crystals. In the coadsorption studies, it is interesting that the TPD exhibit N_2 desorption features which are similar in shape to those observed on Rh/ceria (*12, 19*). Although adsorbed oxygen has been shown to significantly inhibit NO adsorption on other Rh surfaces, the TPD results on Rh/ceria could be consistent with a relatively low oxygen coverage of ~25% of a monolayer. Since the entire surface is affected, the oxygen would have to be adsorbed evenly over the entire Rh surface. Alternatively, if the oxygen is just below the surface of the Rh particles, NO may still adsorb but the rates of reactions which remove N_2 from the surface, both $NO_{ad} + N_{ad} \rightarrow N_2 + O_{ad}$ and $2N_{ad} \rightarrow N_2$, should still be modified significantly. Subsurface oxygen may also be available for reaction with CO, so that the NO and CO results would still be consistent.

DISCUSSION

Previous studies have demonstrated that the oxygen in cerium oxide is involved in the emissions-control reactions and can exchange with reactants (*7, 22*). However, to our knowledge, this is the first evidence that oxygen can actually migrate from the oxide onto Rh particles at relatively low temperatures. The results of previous work could be interpreted as being due either to reaction at the interface between the particles and oxide or to gas-phase transport of species between the metal and oxide phases. Our results show that the entire surface of even large, supported Rh particles appears to be modified by the presence of oxygen.

Our results can also help explain the high activity of Rh/ceria catalysts for the water–gas-shift reaction. Schlatter and Mitchell reported that Rh/ceria catalysts exhibit a much higher activity for this reaction than either Rh or ceria alone under transient conditions (*7*). It is easy to rationalize this observation based on our results. The oxygen from cerium oxide can migrate to the Rh surface, making it available for reaction with CO to form CO_2. Since ΔG for the reaction $Ce_2O_3 + H_2O = 2CeO_2 + H_2$ is negative at temperatures of interest for catalysis, the partially reduced ceria can be readily reoxidized by water, completing the catalytic cycle.

The driving force for migration of oxygen from ceria to Rh is not clear since thermodynamic considerations show that bulk Rh cannot be oxidized by ceria under the conditions of our experiment. The Gibbs free energy of the most probable reaction, $Rh + 2CeO_2 = RhO + Ce_2O_3$, is +66 kcal/mol at 298 K, so that the equilibrium should be shifted far to the left. This calculation does not take into account possible changes in the energetics due to the surface or to contact between the Rh and the ceria, but one should certainly not expect to see bulk oxidation of the Rh by CeO_2. Furthermore, the migration of oxygen is not a property of ceria alone but must be related to how Rh and ceria interact, since oxygen migration is strongly affected by the specific metal which is being supported by ceria. In the case of Pt/ceria, we did not find any evidence for oxygen migration onto the Pt in our model catalysts, nor did Schlatter and Mitchell observed an increase in the water–gas-shift activity of Pt/ceria over that measured on ceria alone. While CO_2 formation was reported in one TPD study of CO on Pt/ceria catalysts (*22*), this study was carried out on high-surface-area materials so that desorption was shifted to considerably higher temperatures (*23, 24*). This probably indicates that oxygen migration can occur from ceria to Pt but that the rates are much lower than on Rh/ceria.

A clue as to how the oxygen migrates may be found in the low dispersion that was measured for Rh on ceria in our study. The average particle sizes estimated from CO adsorption on Rh were twice the value found for the same metal coverage for Pt. As mentioned earlier, it is tempting to suggest that the Rh surfaces are partially covered with ceria after heating in a manner similar to that which has been suggested for LaO_x on Pd (*14*). If oxide species could partially spread onto the metal, one might expect that oxygen could migrate through these entities and create a larger interface between the oxide and the metal at which CO could interact. Obviously, further work will be needed to confirm or disprove this mechanism for oxygen migration.

SUMMARY

Evidence has been found that oxygen from CeO_2 can migrate onto Rh and react with adsorbates on the Rh beginning at ~400 K. This interaction between ceria and Rh is not found for Pt/ceria catalysts, indicating that the interactions between ceria and Rh are specific interactions between the metal and the oxide. These results help to explain the high activities of Rh/ceria catalysts for the water–gas-shift reaction.

ACKNOWLEDGMENTS

This work was supported by the DOE, Basic Energy Sciences, Grant DE-FG03-85-13350. Support for the electron microscopy experiments was partially provided by the NSF, MRL Program, Grant DMR 88-19885. We also thank E. Delikouras and D. D. Perlmutter for their assistance in preparing ceria films.

REFERENCES

1. Yao, H. C., and Yu Yao, Y. F., *J. Catal.* **86,** 254 (1984).
2. Su, E. C., Monteuil, C. N., and Rothschild, W. C., *Appl. Catal.* **17,** 75 (1985).
3. Herz, R. K., *Ann. Chem. Soc. Symp. Ser.* **178,** 59 (1982).
4. Summers, J. C., and Ausen, S. A., *J. Catal.* **58,** 131, (1979).
5. Zhou, Y., Nakashima, M., and White, J. M., *J. Phys. Chem.* **92,** 812 (1988).
6. Hindin, H. G., U.S. Patent 3,870,455 (1975).
7. Schlatter, J. C., and Mitchell, P. J., *Ind. Eng. Chem. Prod. Res. Dev.* **19,** 288 (1980).
8. Kim, G., *Ind. Eng. Chem. Prod. Res. Dev.* **21,** 267 (1982).
9. Su, E. C., and Rothchild, W. G., *J. Catal.* **99,** 506 (1986).
10. Zafiris, G. S., and Gorte, R. J., *Surf. Sci.* **276,** 86 (1992).
11. Zafiris, G. S., and Gorte, R. J., *J. Catal.* **132,** 275 (1991).
12. Altman, E. I., and Gorte, R. J., *J. Catal.* **113,** 185 (1988).
13. Altman, E. I., and Gorte, R. J., *Surf. Sci.* **195,** 392 (1988).
14. Underwood, R. P., and Bell, A. T., *Appl. Catal.* **34,** 289 (1987); Rieck, J. S., and Bell, A. T., *J. Catal.* **99,** 278 (1986).
15. Root, T. W., Schmidt, L. D., and Fisher, G. B., *Surf. Sci.* **150,** 173 (1985).
16. Baird, R. J., Ku, R. C., and Wynblatt, P., *Surf. Sci.* **97,** 346 (1980).
17. Ko, C. S., and Gorte, R. J., *Surf. Sci.* **161,** 597 (1985).
18. Thiel, P. A., Williams, E. D., Yates, J. T., and Weinberg, W. H., *Surf. Sci.* **84,** 54 (1979).
19. Root, T. W., Schmidt, L. D., and Fisher, G. B., *Surf. Sci.* **134,** 30 (1983).
20. Ho, P., and White, J. M., *Surf. Sci.* **137,** 103 (1984).
21. Villarubia, J. S., and Ho, W., *J. Chem. Phys.* **87,** 750 (1987).
22. Jin, T., Okuhara, T., Mains, G. J., and, White, J. M., *J. Phys. Chem.* **91,** 3310 (1987).
23. Gorte, R. J., *J. Catal.* **75,** 164 (1982).
24. Demmin, R. A., and Gorte, R. J., *J. Catal.* **90,** 32 (1984).
25. Palmberg, P. W., Riach, G. E., Weber, R. E., and MacDonald, N. C., "Handbook of Auger Electron Spectroscopy." Physical Electronics Industries, Eden Prairie, MN, 1972.